Direct Air Capture with Amino Acid Solvent: Operational Optimization using a Crossflow Air-Liquid Contactor[1]

Keju An[a], Kai Li[a], Cheng-Min Yang[a], Jamieson Brechtl[a], Diana Stamberga [b], Mingkan Zhang[a], Kashif Nawaz[a]

[a]Buildings and Transportation Science Division, Oak Ridge National Laboratory, 1 Bethel Valley Road, Oak Ridge, TN, USA

[b]Chemical Science Division, Oak Ridge National Laboratory, 1 Bethel Valley Road, Oak Ridge, TN, USA

Abstract

Direct air capture (DAC) is a negative emission technology for removing CO_2 from the atmosphere to maintain the CO_2 level within a reasonable range so as to address greenhouse effects. In this study, the operational optimization of lab-scale DAC has been investigated using a crossflow air-liquid contactor loaded with a three dimensionally printed Gyroid packing structure and a potassium sarcosinate solvent. The effects of various parameters, including feed air flow rate, liquid solvent flow rate, contactor geometry, and ambient temperature, are examined. The results demonstrate that the Gyroid packing design achieves comparable CO_2 capture performance to conventional packed beds but with a significantly lower pressure drop of up to 77.8%, suggesting its potential as an efficient and cost-effective solution for gas-liquid contactors in DAC. Additionally, the study explores the climate impact on CO_2 capture performance and finds that as the air temperature increases from 35°F to 95°F at fixed relative humidity at 80%, the CO_2 capture rate increased from 23.2 to 46.8% with better stability. The research highlights the importance of optimizing contactor design and operational conditions to improve the CO_2 capture rate and feasibility of DAC systems as a negative emission technology for addressing greenhouse effects.

Keywords: Direct Air Capture, CO_2 Capture Capacity, Contactor Design, Potassium Sarcosinate, Weather Condition

1. Introduction

As more nations pledge to achieve net zero emissions, policymakers are increasingly focusing on translating these commitments into tangible policy actions and strategies. Currently, only a limited number of countries and companies have developed detailed plans or pathways to reach their net zero goals[1]. Carbon capture, storage, and utilization (CCSU) are widely acknowledged as significant components for addressing global warming. To achieve significant reductions in atmospheric CO_2, a wide range of technologies are required, including capturing emissions from specific sources and removing CO_2 directly from the atmosphere[2-4]. Negative emissions technologies (NETs) play a crucial role in reducing CO_2 levels by extracting CO_2 from the atmosphere. Direct air capture (DAC), bioenergy with carbon capture and storage, ocean fertilization, and afforestation are four prominent approaches to achieving negative emissions[3, 4]. NETs, particularly

DAC, are essential elements of a comprehensive response to climate change, offering diverse solutions to tackle the challenge. By promoting transparency and integrating carbon dioxide removal (CDR) into net zero strategies, policymakers can identify the technological, policy, and market needs within their jurisdictions while enhancing public understanding of these approaches.

DAC employs chemical processes to directly extract CO_2 from the atmospheric air. Although DAC shows promise in terms of scalability, modularity, and the ability to utilize arid land, it currently remains costly, considering the dollars required per tonne of CO_2 removed[5, 6]. Nevertheless, DAC offers notable advantages as a CDR option, including its ability to achieve high storage permanence when coupled with geological storage and its minimal impact on land and water resources[7]. Additionally, the captured CO_2 can be used, such as in food processing or in combination with hydrogen to generate synthetic fuels. As the transition to net zero emissions continues, the CO_2 used for synthetic fuel production would increasingly need to be sourced from sustainable bioenergy sources or directly extracted from the atmosphere. This approach is crucial in order to avoid delayed emissions from CO_2 derived from fossil fuels when the synthesized fuel is burned[8, 9]. Hence, DAC emerges as a viable option to achieve this objective.

Among the various DAC technologies, solvent-based absorption is considered one of the most advanced and well-established methods. In conventional solvent-based absorption systems, a solution of CO_2-absorbing solvent is introduced into a packed column, where it comes into contact with the dilute CO_2 present in the air. The gaseous CO_2 is absorbed into the liquid solvent, resulting in an outlet stream with reduced CO_2 concentration and a liquid stream that is rich in CO_2. To enhance the contact between the gas and liquid phases, structured packing is often employed in solvent-based systems, providing a large interfacial area for efficient interaction between the dilute CO_2 and the liquid solvent. The performance of CO_2 capture in solvent-based approaches largely relies on the characteristics of the packing material, which facilitates the contact and reaction between the dilute CO_2 and the solvent[10]. In previous studies, conventional structured packing designs such as stainless steel[11, 12] and PVC[13, 14] have been utilized for liquid solvent-based DAC systems although there have been limited advancements and changes. The capital cost associated with packing and the column itself typically constitutes around 75% of the total costs, which is primarily determined by the column size and the amount of packing[15]. However, advancements in structured packings have the potential to significantly reduce capital costs and energy requirements by minimizing the column size and packing volume[6, 16, 17]. Recent research has focused on exploring the use of advanced packing columns specifically tailored for DAC applications[10, 18].

This study investigates the design of a gas-liquid contactor with a large surface area for the chemical absorption of CO_2 from air using an aqueous potassium sarcosinate (K-SAR) solutions. Previous research has shown that aqueous basic salts of amino acids hold promise for DAC applications[18-21]. In recent years, aqueous amino acid salt solutions, particularly K-SAR, have garnered attention as superior alternatives to conventional amine solvents. These solutions offer several advantages such as higher loading capacities, faster CO_2 absorption kinetics, lower volatility and corrosivity, and greater chemical stability. This research paper focuses on the development of a high surface area gas-liquid contactor for the chemical absorption of CO_2 from ambient air using aqueous amino acid solutions containing K-SAR.

In this work, we propose a framework to create, manufacture, and experimentally evaluate advanced packing geometries based on a Gyroid design with a triply periodic minimal surface (TPMS) structure. TPMS structures consist of two interpenetrating fluid domains separated by a thin wall, exhibiting periodic properties in all three dimensions[22]. These nature-inspired surfaces minimize area, possess zero mean curvature, and offer smooth paths for fluid flow. Prior investigations have demonstrated that TPMS geometries can improve mass transfer performance by 49-61% and increase effective gas-liquid interfacial area by 91-140% compared to conventional packing materials like Mellapak 250.Y[10]. In this study, we

evaluated the CO_2 capture performance of a Gyroid geometry with an advanced structured packing and compared it to a conventional packed bed packing using polypropylene balls of different sizes. Three dimensionally (3D) printed Gyroid packing structure tested with varying air flowrates and solvent conditions to determine the optimal operational parameters. Then, the Gyroid packing test was performed in an environmental chamber under different temperature and humidity conditions to check its climate impact in terms of CO_2 capture performance.

2. Experimental Setup

2.1. Packing structure for air contactor

In the current study, a modular absorber device on a liter-scale was employed to assess the efficiency of packing materials in capturing CO_2 from ambient air using an aqueous 1M K-Sar solution (a mixture of potassium hydroxide and sarcosine). We investigated novel packing geometries for CO_2 capture from ambient air by employing 3D-printed structures known as TPMS with a Gyroid pattern. A comparative analysis was conducted between the Gyroid-structured packing and conventional packings composed of polypropylene balls of different sizes. The Gyroid packings demonstrated comparable or enhanced maximum fluid capacity and pressure drops compared to traditional packings, indicating their potential suitability for industrial applications.[10].

The Gyroid structure's geometric design was generated using the open-source software MSLattice, allowing for precise control over the desired thickness and unit length of each layer. Subsequently, STL (Stereo Lithography) files were generated using MSLattice to represent the Gyroid structure. The specimens were designed as Gyroid unit cells, with a total of seven unit cells per side length, resulting in a configuration measuring $3 \times 2 \times 2$ in^3. To fill the $4 \times 4 \times 6$ in^3 air contactor, eight 3D-printed specimens were produced. The Stratasys Fortus 450 printer was utilized for the 3D printing process, with each layer of the Gyroid structure having a thickness of 0.01 in. Stratasys water was used to dissolve the support structure within the printed part. ABS-30m was chosen as the material for the Gyroid structure due to its remarkable resistance to heat, cold, and chemicals, making it a crucial contributor to the advancement and proliferation of three-dimensional printing technology[23].

Figure 1 (a) provides visual representations of the packed beds comprising polypropylene particles, showcasing side and top views for three different particle diameters: 1/4 in, 5/16 in, and 3/8 in. In Figure 1 (b), the 3D-printed Gyroid packing, created using ABS-30m material, is presented from both the side and top perspectives. For a comprehensive overview of the various packing types, Table 1 offers a comparative analysis between the polypropylene balls and the 3D-printed Gyroid structure. Notably, the specific surface area (SSA) of the 3D-printed Gyroid structure, intentionally set at 579 m^2/m^3, is specifically compared to the smallest polypropylene packing (3/8 in) with a SSA of 578 m^2/m^3. A notable distinction between Gyroid packing and the packing with the smallest polypropylene (3/8 in) is the significantly higher voidage observed in the Gyroid structure. This disparity arises from the Gyroid's flexible design, which allows for adjustments of various functional parameters such as unit cell size, wall thickness, and curvature. The higher voidage offers increased open space within the packing material, potentially enhancing gas-liquid contact and improving mass transfer efficiency during CO_2 capture processes[24]. This information highlights the subtle differences in SSAs between the two packing types, emphasizing the potential advantages offered by the Gyroid structure in terms of surface area-to-volume ratio and its potential impact on CO_2 capture efficiency.

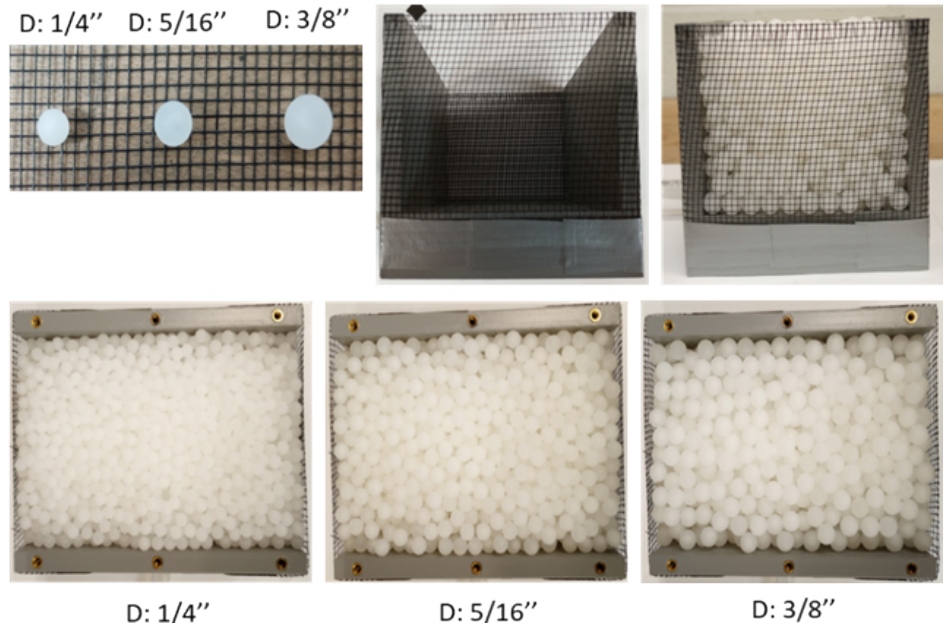

(a)

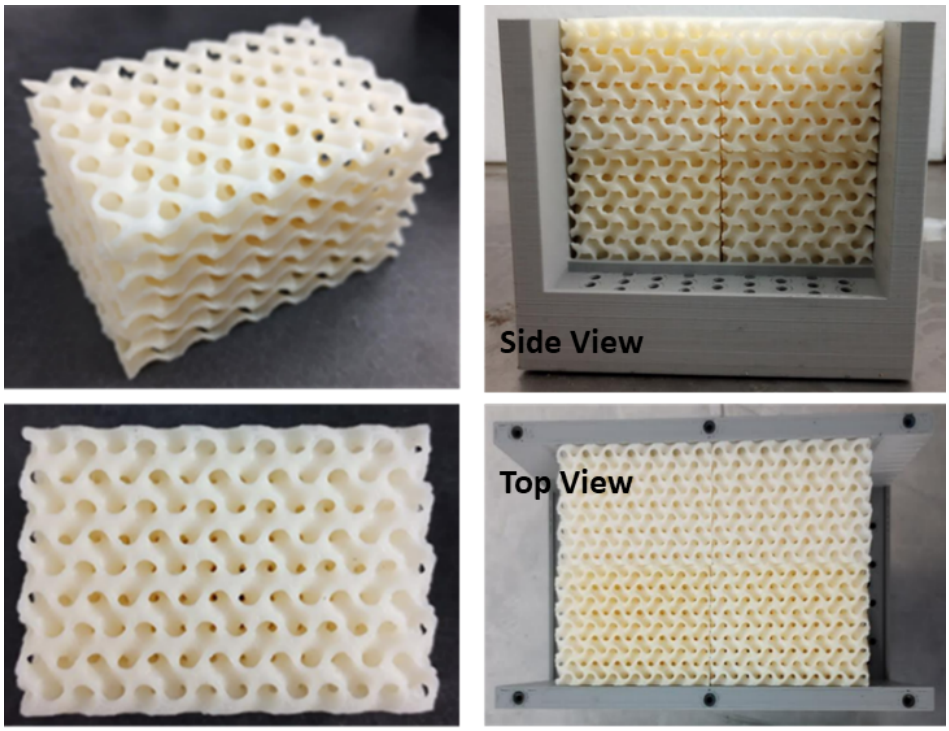

(b)

Figure 1. Packing types: (a) conventional packed bed by polypropylene balls, (b) 3D printed Gyroid.

Table 1. Specifications of each packing types for DAC application.

	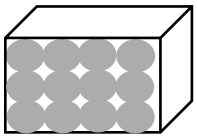 Packed bed #1	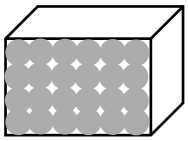 Packed bed #2	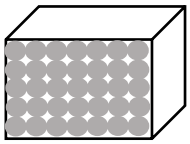 Packed bed #3	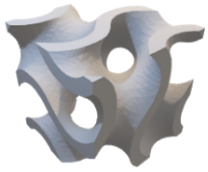 Gyroid
Particle size/Unit cell size (in)	0.375	0.312	0.25	0.42
Voidage (%)	40.3	39.4	38.7	70
Total number of balls/unit cells	1,615	2,981	5,706	1,052
Specific surface area (m^2/m^3)	360	438	578	579
Actual surface area (m^2)	0.46	0.56	0.71	0.71

2.2. Solvent preparation and characteristics

The required chemicals, namely sarcosine (99% purity) and potassium hydroxide pellets (99% purity), were procured from Sigma Aldrich. To prepare a 1M K-SAR solution, a mixture of 89.1 g sarcosine and 56.1 g KOH was added to a 1-liter solution of deionized water. Mixing the components resulted in the formation of a 1-liter volume of 1M K-SAR solution. One of the key advantages of using amino acid solutions for CO_2 capture is the ability to regenerate the loaded solution. The dynamic viscosity, μ, and density, ρ, of 1M K-Sar are 0.01 kg/m-s and 1100 kg/m_3 respectively. The governing chemical reaction with atmospheric gas phase CO_2 and 1M K-Sar are shown in Equations 1 and 2. Regeneration is achieved by directly applying heat to the fluid, which facilitates the desorption of CO_2 and restores the amino acid to its basic form. This study explores the potential of utilizing aqueous amino acid solutions, specifically K-SAR, for CO_2 capture. The unique properties and regenerability of these solutions make them promising candidates for sustainable carbon capture technologies.

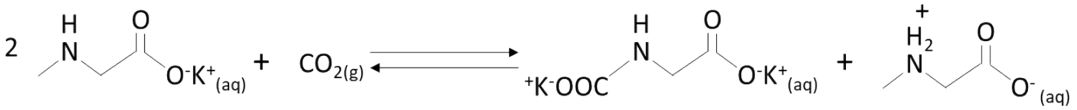

(1)

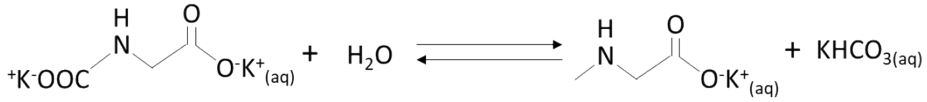

(2)

2.3. Air contactor design and wind tunnel application

The design of the air contactor involves the implementation of a horizontal air flow that passes through the contactor. In this particular setup, a micro- to millimeter thickness layer of liquid sorbent is applied to a vertical packing material[24]. The design of a crossflow air contactor for this purpose is influenced by factors such as gas-solvent contact, solvent flow rate, and energy requirements[13, 28]. High surface area packing structures are utilized to enhance the interaction between the gas and liquid phases. Typically, stainless steel is used in conventional cooling tower packing structures. However, employing advanced packing structures potentially reduces the pressure drop across the contactor that can result in lower operational costs[10]. To optimize solvent flow rate and packing structure coverage while minimizing capital and operational expenses, the Gyroid packing has been proposed. The energy requirements associated with cross-flow contactors arise from the pumping of the solvent and the operation of fans to overcome the pressure drop across the contactor. For an annual capture rate of 1 Mt CO_2 per year, these contactors are estimated to be 20 m tall, 200 m long, and have a depth ranging from 5 to 8 m[14]. The depth directly affects the pressure drop across the contactor and the percentage of CO_2 captured from the inlet air stream, making its impact on total energy requirements complex.

Liquid solvent-based CO_2 absorption in structured packings was conducted using a modular absorber column that combined 3D-printed components with different packing structures. The purpose of this setup was to achieve the efficient absorption of CO_2. To ensure an even distribution of the solvent flow throughout the system, a specially designed top distributor was created. This distributor, which is featured in Figure 2(a), was 3D-printed and incorporated evenly spaced circular orifices at the top of the liquid flow inlet. Each orifice was designed to have a height of 0.2 in, allowing the liquid solution to collect at the top and smoothly flow down through the distributor.

Figure 2(b) shows the 3D-printed contactor containing Gyroid packing, which was specifically chosen for the wind tunnel experiment. Gyroid packing is renowned for its substantial surface area and effective gas-liquid contact, thereby optimizing the absorption process. To assess the performance of the structured packings, a fixed volume of recirculated aqueous Amino Acid solvent (1M K-Sar, a mixture of Potassium Hydroxide and Sarcosine) was employed for CO_2 removal from the surrounding ambient air. A consistent volume of 1.5 liters of the solvent was used, and a continuous recirculation system was implemented. The liquid residue was collected in a designated container and subsequently pumped back to the top of the distributor, ensuring continuous flow and enhanced gas-phase interaction for improved CO_2 absorption.

CO_2 capture rates are observed at different ranges of air flow rates and solvent flow rates to find the optimum operating conditions. The CO_2 capture rate is calculated based on Equation 3:

$$CO_2\ Capture\ Rate = \frac{CO_{2,upstream}\,[ppm]\ - CO_{2,downstream}\,[ppm]}{CO_{2,upstream}\,[ppm]} \quad (3)$$

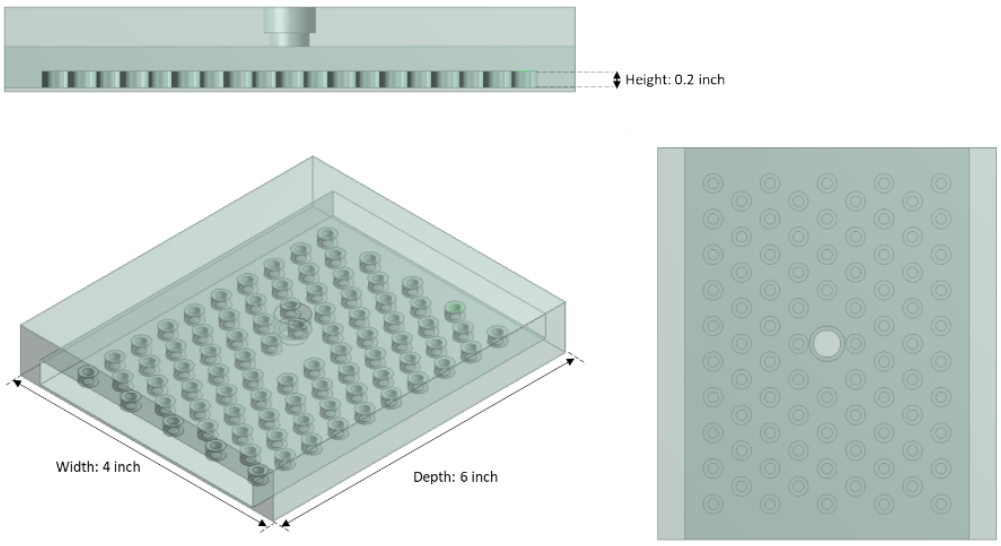

(a)

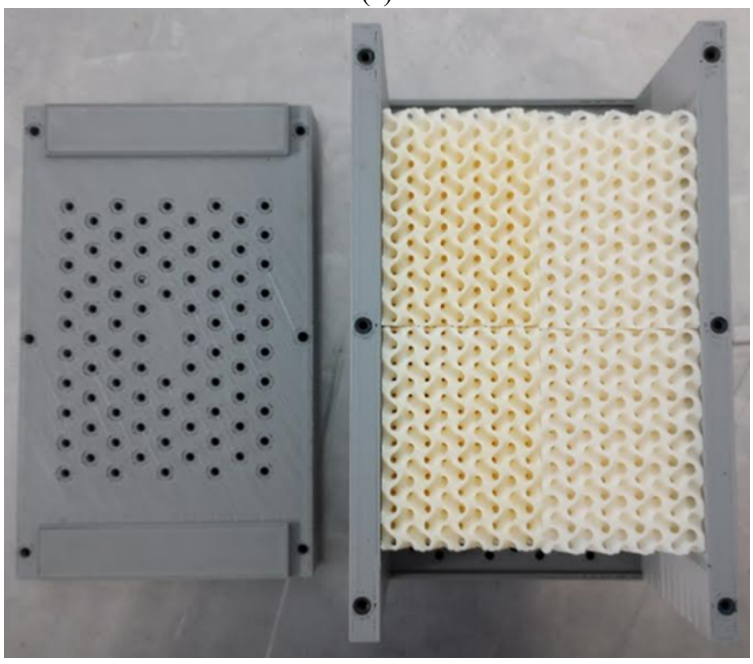

(b)

Figure 2. Liquid-solvent (a) distributor CAD design and (b) 3D-printed contactor with Gyroid packing for wind tunnel experiment.

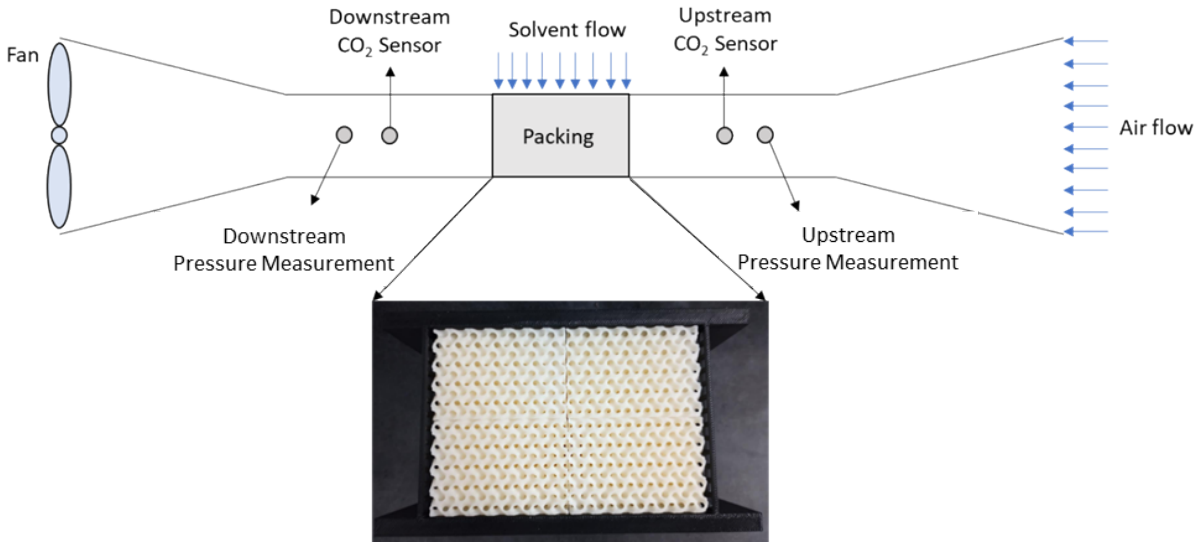

(a)

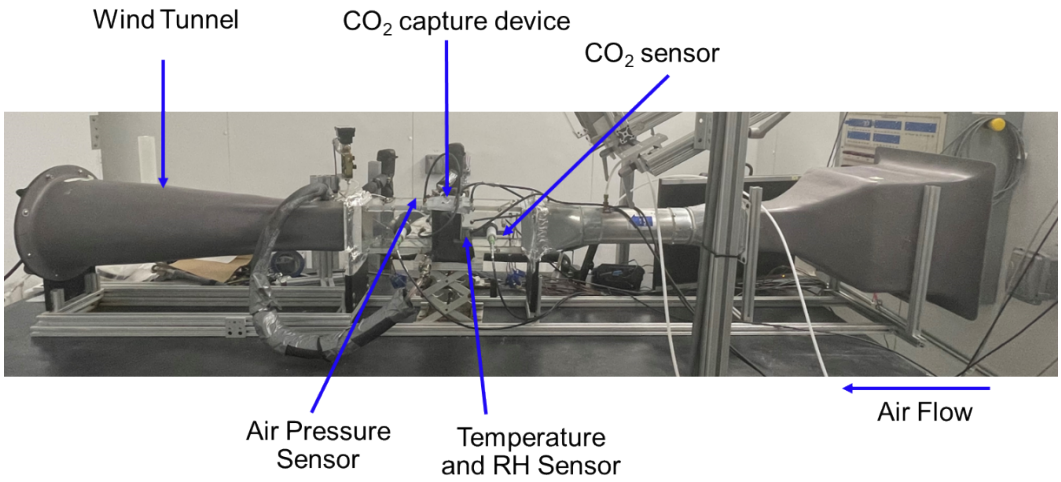

(b)

Figure 3. (a) Experimental Schematic and (b) Wind tunnel setup for the DAC application experiment.

To ensure precise control over air temperature and humidity, a controlled environment was established by an environmental chamber. The wind tunnel served as the primary experimental setup for investigating the CO_2 capture performance of different packing types. Situated at the center of the wind tunnel, the various packings were subjected to airflow generated by a downstream fan. A distributor was employed to deliver the 1M K-Sar liquid solvent from the top of the air contactor to the packing, facilitating the gas-liquid interaction. Throughout the experiment, monitoring of the chamber's temperature and humidity levels was conducted to ensure consistency and control. To regulate the mass flowrate of the liquid solvent, a ball valve was utilized. Additionally, a differential pressure transducer was employed to measure the pressure drop across the air contactor, as indicated in Figure 3. The gaseous effluent from the absorber was directed to an Omega digital mass flowmeter, while a portion of it was supplied to an infrared CO_2 sensor (Vaisala GMP252). These instruments facilitated the measurement and analysis of upstream and downstream CO_2

concentrations within the system, providing valuable data for the evaluation of the CO_2 capture performance of the different packing materials.

3. Results and Discussion

In accordance with the outlined methodology, the wind tunnel setup (Figure 3) was utilized to conduct experiments comparing the CO_2 capture performance of conventional packed beds and 3D-printed Gyroid packings. Initially, the focus was on evaluating and discussing the optimal operational conditions of conventional packed beds with varying ball sizes and flowrates of solvent and air, emphasizing their CO_2 capture efficiency. Subsequently, a comprehensive comparison was made between the CO_2 capture performance of the conventional packed bed and the Gyroid packing. Through careful analysis and discussion, the relative effectiveness of these two packing types was assessed, providing valuable insights into their respective capabilities. Furthermore, the CO_2 capture performance of the Gyroid packing was investigated under diverse climatic conditions. The overall operational conditions of the wind tunnel experiment are displayed in Table 2.

Table 2. Operational range of DAC experimental condition.

Air Flowrate (LPS)	0.6 to 3.4
Solvent Flowrate (GPM) (in LPS)	0.06 to 0.16 0.00378 to 0.0101
Temperature (°F)	35, 65, 95
Relative Humidity	80%
Specific surface area (m^2/m^3)	360 to 579
Actual surface area (m^2)	0.46 to 0.71

3.1. Determining the Optimal Operational Parameters for Conventional Packings

Three different ball sizes were employed in conventional packed beds to investigate the impact of SSA on CO_2 capture rate performance. The ball sizes used were 0.25, 0.312, and 0.375 in, corresponding to SSA of 578, 457, and 375 m^2/m^3 (Table 1), respectively. Figure 4 illustrates the results obtained for the CO_2 capture rates of the three packed beds. The contour plots presented in the results were obtained from a dataset comprising 30 data points. Each data point represents the average values over a 3-minute interval. These data points were utilized to create the contour plots, which provide a visual representation of the variations and trends observed in the parameters being analyzed. Figure 4 reveals that packings with the two larger

ball sizes (0.312 and 0.375 inches) exhibited similar CO_2 capture performance across the range of 0.5-3.5 LPS air flowrate and 0.06-0.16 GPM solvent flowrate. These packings demonstrated CO_2 capture rates ranging from 5% to 25%, primarily dependent on the air flowrate rather than the solvent flowrate. In contrast, the conventional packing with the smallest ball size (corresponding to a SSA of 578 m^2/m^3) displayed significantly higher CO_2 capture rates, particularly at lower air flowrates, reaching above 50%. For instance, at air flowrates below 1 LPS and with a wide range of solvent flowrates between 0.09 and 0.16 GPM, the CO_2 capture rate exceeded 45%. However, at higher air flowrates, the influence of solvent flowrate became more significant in terms of CO_2 capture rate.

Figure 5 provides a comprehensive depiction of the CO_2 concentrations, both upstream and downstream, under two distinct testing conditions. The representative scenarios were chosen as: 1) Air flowrate: 1 LPS & Solvent flowrate: 0.12 GPM, and 2) Air flowrate: 2 LPS & Solvent flowrate: 0.12 GPM. The selection of these conditions was based on the observed stronger influence of air flowrate on the CO_2 capture rate, compared to the solvent flowrate. The results presented in Figures 5(b) and 6(c) pertain to a packed bed characterized by a SSA of 578 m^2/m^3. The testing was conducted over a duration of 5 hours, and the obtained outcomes are shown in Figures 5(b) and 6(c).

Examining the first testing condition (Air flowrate: 1 LPS & Solvent flowrate: 0.12 GPM), it can be observed that the CO_2 capture rate exhibited variability, ranging from 44% to 50% after a stabilization period of 10 minutes for both upstream and downstream CO_2 concentrations. In contrast, the second testing condition which features a two-fold increase in air flowrate displayed a relatively lower capture rate that ranged from 27% to 31% over the entire 5-hour test duration. These findings underscore the critical role of air residence time in achieving optimal CO_2 capture performance. Prior research has indicated that increasing the depth of the air contactor can lead to capture rates as high as 75%, facilitated by higher incoming air velocities of 1.4 m/s (equivalent volumetric flowrate, 0.0036 m^3/s) [14]. However, it is essential to consider tradeoffs in the design process, such as the potential impact on pressure drop and the additional capital costs associated with modifying the contactor to accommodate the extended travel length of the air flow[29-31]. Addressing these considerations is crucial for achieving an optimal balance between CO_2 capture performance and the associated operational and economic considerations.

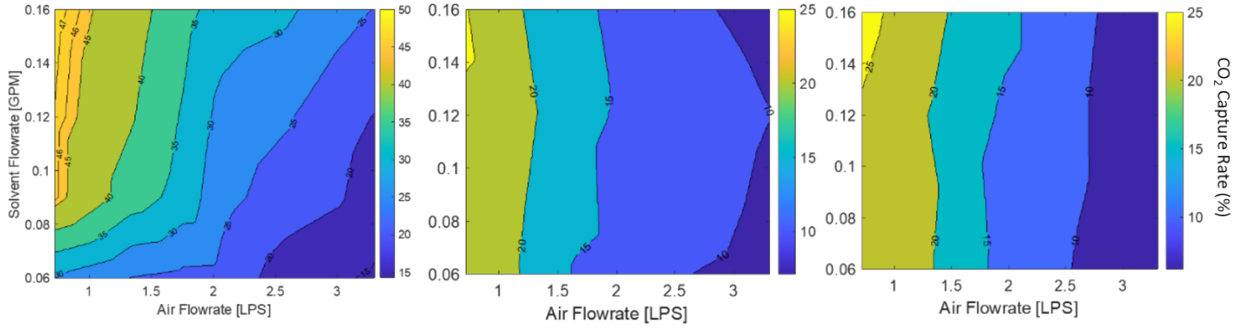

(a) (b) (c)

Figure 4. CO_2 capture rate for varying air flowrates and solvent flowrates (a) SSA: 578 [m^2/m^3] (b) SSA: 457 [m^2/m^3] (c) SSA: 375 [m^2/m^3].

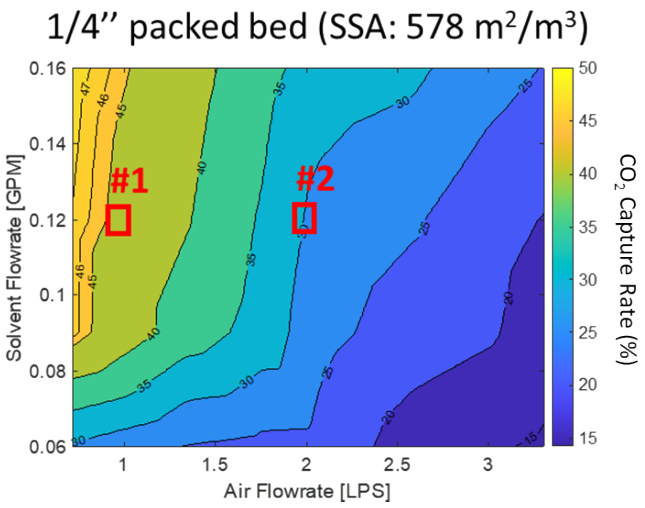

(a)

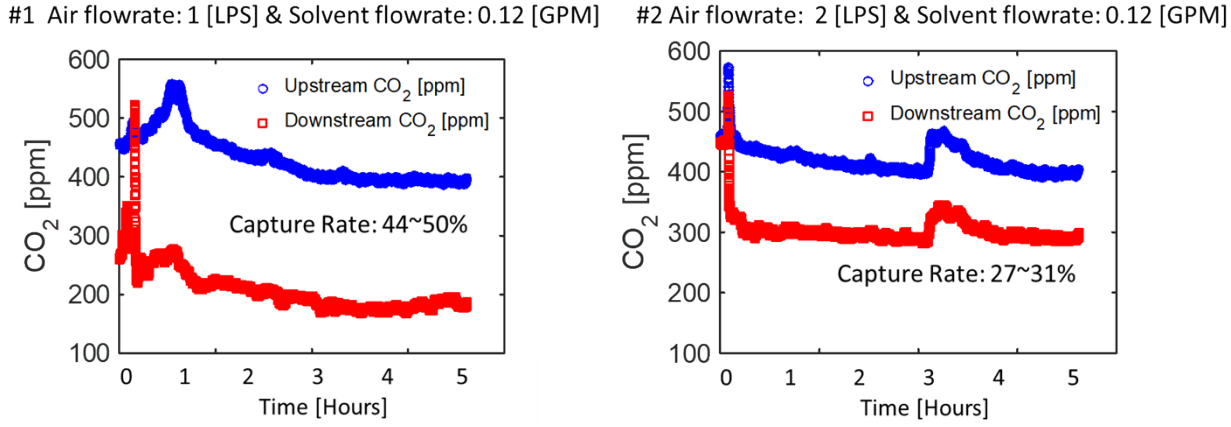

(b) (c)

Figure 5. 5-hour testing at two different test conditions: (a) two representative experimental conditions (b) CO_2 upstream and downstream concentration at location #1, (c) CO_2 upstream and downstream concentration at location #2 using conventional packing with a SSA of 578 m^2/m^3.

3.2. Advantage of advanced Gyroid packing

We developed and manufactured the Gyroid packing using ABS-30m material to replicate the SSA of a conventional packed bed, which was 578 m^2/m^3. Initially, we conducted tests within the same solvent and air flowrate range, ranging from 0.06 to 0.16 GPM and 0.5 to 3 LPS, respectively, to assess the CO_2 capture performance and make a comparison with the conventional packed bed. Figure 6 illustrates the CO_2 capture rate and pressure drop of the conventional packed bed (SSA: 578 m^2/m^3) and the Gyroid packing (SSA: 579 m^2/m^3).

The overall CO_2 capture performance of the Gyroid packing appears to be similar to that of the conventional PP ball packing. However, significant differences were observed in the lower solvent flowrate range below 1 GPM. In this range, the Gyroid packing exhibited a higher CO_2 capture performance compared to the conventional PP ball packing. For instance, at an air flowrate of 1.5 LPS and a solvent flowrate of 0.06 GPM, the Gyroid packing achieved a 30.5% CO_2 capture rate, which was 20% higher than the conventional

PP packing's CO_2 capture rate of 24.4%. Similarly, at an air flowrate of 2 LPS and a solvent flowrate of 0.06 GPM, the Gyroid packing showed a 26.8% CO_2 capture rate, surpassing the conventional PP packing's CO_2 capture rate of 22.4% by 16.4%. These results can be attributed to the material's surface tension and the fluid dynamic behavior at the interface between the liquid film and the CO_2 gas phase in the air. The surface energy of the material is a critical parameter influencing the wetting efficiency on the column layer surface[10, 24]. As anticipated, the ABS-30m material exhibited a 20.7% higher surface energy (38.5 mJ/m^2) compared to the critical surface energy of the conventional PP packed bed (30.5 mJ/m^2). Consequently, the contact angles were measured at 80.9° (hydrophilic) and 102.1° (hydrophobic) for ABS-30m and conventional PP, respectively[32].

Another notable result is the pressure drop across both types of packing throughout the entire range of air flowrates, which was from 0.5 to 3 LPS. A common tradeoff and optimization point in liquid absorption is the balance between packing surface area and air flowrate. Increasing either parameter enhances the CO_2 capture rate but also leads to increased pressure drop. As shown in Figure 6, as the air flowrate increased while maintaining a fixed SSA, the pressure drop rose for both packing types. However, across all air flowrates, the Gyroid packing exhibited 33% to 77.8% lower pressure drop compared to the conventional PP packing. This finding aligns with previous studies involving ceramic foams and spherical meshes, as well as 3D printed packing which also demonstrated reduced pressure drop[33-36]. The impact of air movement by fans can be significant. According to a previous study on fan power in relation to pressure drop[12], fan power is directly proportional to pressure drop. This means that the Gyroid packing structure has the potential to reduce operational fan power by 33% to 77% in the air contactor unit. Nevertheless, there are limitations due to factors such as the capital cost of mass production of 3D printed advanced packing, raw material expenses, and the duration of post-processing. The packings differ considerably from each other in terms of cost or pressure drop per unit length, necessitating careful consideration of column height and air flowrates to achieve a balance between the two factors.

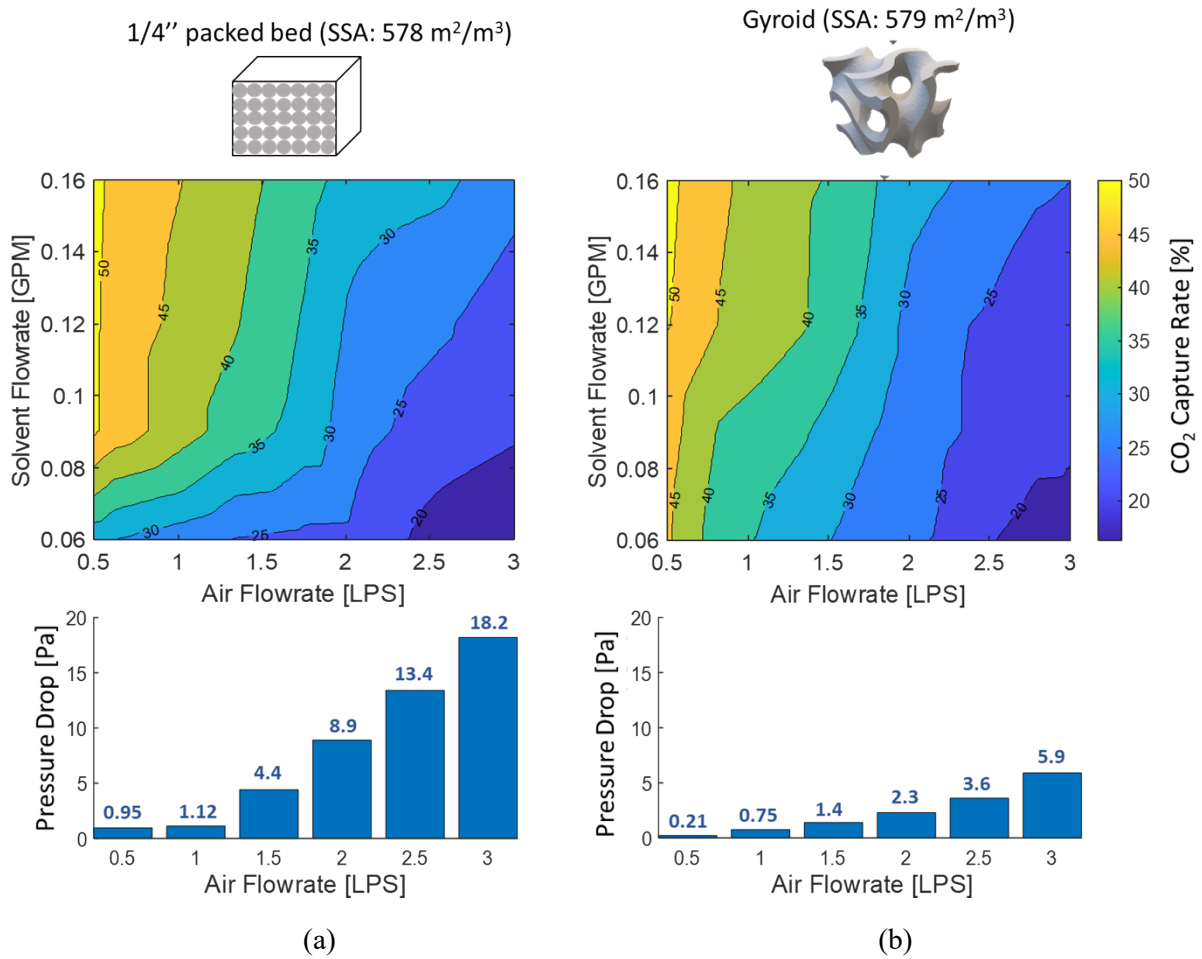

Figure 6. CO_2 capture rate and pressure drop of (a) conventional packed bed (SSA: 578 m^2/m^3) and (b) Gyroid packing (SSA: 579 m^2/m^3).

3.3. Climate impact on CO_2 capture performance

In this study, the impact of different climatic conditions on the CO_2 capture performance of the advanced Gyroid packing structure was investigated. The experiments were conducted under fixed operational conditions, including an air flowrate of 1 LPS and a solvent flowrate of 0.12 GPM. Three distinct climatic conditions were considered, namely 35°F, 65°F, and 95°F, with a fixed relative humidity of 80% to minimize water evaporation during the experiments. Each climatic condition was tested for a duration of 1 hour, with data collected at a time resolution of 1 second, resulting in a total of 3,600 data points. The results were analyzed and presented in the form of a whisker plot, as depicted in Figure 7.

The median CO_2 capture rates at the different climatic conditions were observed to be 23.2% at 35°F, 34.9% at 65°F, and 46.8% at 95°F, all at a fixed relative humidity of 80%. It was found that as the atmospheric air temperature increased, the CO_2 capture rates exhibited more stable results. For instance, at an air temperature of 95°F, the CO_2 capture rates were confined within a narrow range of 3.4%. In contrast, at lower temperatures of 65°F and 35°F, the range of CO_2 capture rates increased significantly, with variations of 9.4% and 11.4%, respectively. These findings highlight the influence of climate conditions, particularly

temperature, on the CO_2 capture performance of the Gyroid packing structure, underscoring the importance of considering environmental factors when optimizing and implementing DAC systems.

Previous studies[24, 37] have indicated that the absorption of atmospheric CO_2 into strong aqueous hydroxide solutions is primarily governed by gas-phase resistance and follows a fast pseudo-first-order reaction. The flux of carbon dioxide across the air-liquid interface can be calculated using Equation 4:

$$J_{CO_2} = \sqrt{D_L k[OH^-]}\, K_H C_{CO_2} \qquad (4)$$

where J_{CO_2} represents the flux of CO_2 into the hydroxide solution with a concentration of [OH^-], per unit area per unit time, D_L denotes the diffusivity of CO_2 in the solution, k is the temperature dependant kinetic constant for the reaction of CO_2 with OH^-, K_H is Henry's solubility constant for CO_2, and C_{CO_2} represents the concentration of CO_2 in the air. The units and values at each condition are shared in Table 3. Based on Equation 4 and the properties provided in Table 3, the maximum CO_2 flux at an air temperature of 95°F is calculated to be 7.31E-05 mol/m^2-s, which is 26% higher than the maximum CO_2 flux at an air temperature of 77°F, which is 5.41E-05 mol/m^2-s. The CO_2 capture rate results exhibit a similar trend to the CO_2 flux, with the median CO_2 capture rate at 95°F (46.8%) being 17.9% higher than the median CO_2 capture rate at 77°F (39.6%) based on a linear fit with an R^2 value of 1. This finding suggests a strong correlation between the capture rate and ambient temperature at controlled CO_2 flux.

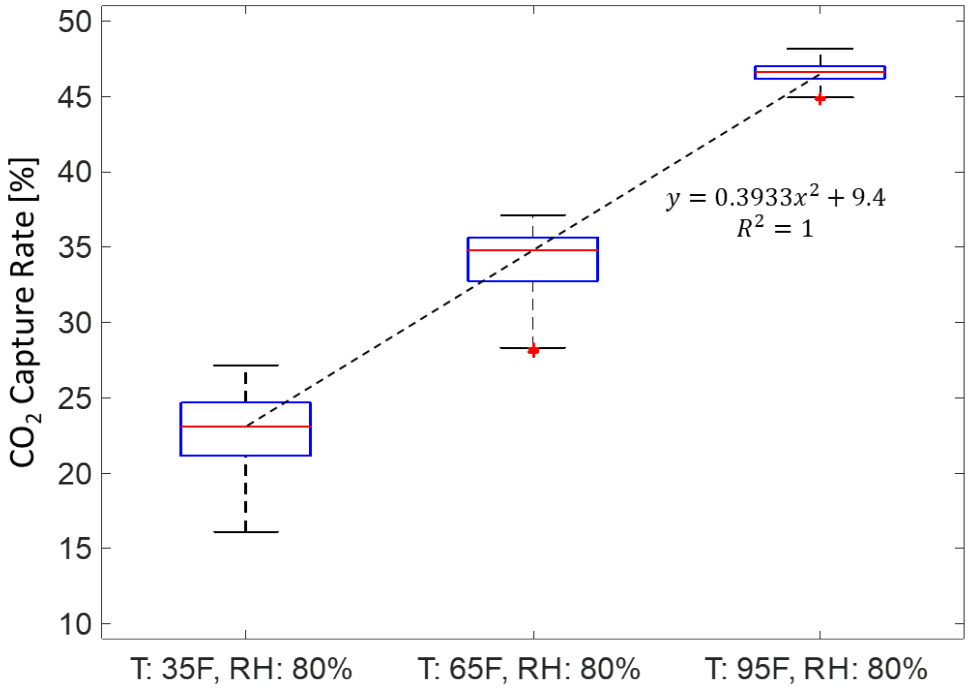

Figure 7. CO_2 capture rate at three different climate conditions: T: 35°F & RH: 80%, 65°F & RH: 80%, 95°F & RH: 80% (with linear fit curve with R^2=1).

Table 3. Properties to calculate CO_2 flux at the air and solution interface.

	T: 25°C (=77°F)	T: 35°C (=95°F)	Reference/Note
D_{L} [m^2/s]	1.54E-09	1.89E-09	[38]
k [L/mol-s]	1.86E+04	4.17E+04	[39]
OH^- [mol/L]	1	1	-
K_{H}	5.46E-01	4.45E-01	[38]
$C_{\mathrm{CO_2}}$ [mol/m^3]	0.0185	0.0185	Equivalent to 415 ppm
$J_{\mathrm{CO_2}}$ [mol/m$_2$-s]	5.41E-05	7.31E-05	-

4. Conclusions

This study focused on optimizing DAC technology using a crossflow air-liquid contactor with a 3D printed Gyroid packing structure and a 1M K-Sar solvent. By investigating various operational parameters, the study aimed to enhance the design and efficiency of DAC systems. The results demonstrated that the Gyroid packing exhibited comparable CO_2 capture performance to conventional packed bed packing, while significantly reducing pressure drop. This finding highlights the potential of the Gyroid design as an efficient and cost-effective solution for gas-liquid contactors in DAC, contributing to the advancement of scalable and sustainable carbon capture systems.

A notable aspect of this study is the use of aqueous amino acid solutions, particularly K-SAR, as solvents for CO_2 capture. These solutions offer advantages over traditional amine solvents, including higher loading capacities, faster absorption kinetics, lower volatility and corrosivity, and greater chemical stability. This study analyzed the climate impact on CO_2 capture performance by subjecting the Gyroid packing to different environmental conditions. The results showed that higher air temperatures led to more stable CO_2 capture rates. This can be attributed to the increased surface energy of the ABS-30m material used in the Gyroid packing, facilitating improved wetting efficiency at the air-solvent interface. Therefore, understanding the influence of climatic conditions on DAC systems is crucial for effective deployment and optimization.

In summary, this study contributes to the advancement of DAC technology by optimizing operational parameters and investigating the potential of advanced packing materials. The Gyroid packing offers comparable CO_2 capture rates (close to 50% at lower air flowrates) to conventional packed bed packing while significantly reducing pressure drop from 33% to 77.8%, indicating its potential as an efficient and cost-effective solution. Our investigation yielded results indicating that the Gyroid packing achieved a similar level of CO_2 capture performance as the conventional packed bed packing, but with a significantly lower pressure drop (3 to 4 times lower). These findings suggest that the Gyroid design holds promise as an efficient and effective solution for gas-liquid contactors in the chemical absorption of CO_2 from air. The Gyroid structure, which is inspired by nature, features periodic surfaces that minimize area and facilitate smooth fluid flow, contributing to its superior performance. Additionally, the Gyroid packing demonstrated resilience and adaptability across different environmental conditions, highlighting its versatility for practical applications. Moreover, considering the climate impact on CO_2 capture performance provides valuable insights for the design and optimization of DAC systems. Lastly, these findings contribute to the development of scalable and sustainable carbon capture solutions, thereby supporting global efforts to address climate change.

Nomenclature

DAC: Direct Air Capture

NET: Negative Emission Technology

CCSU: Carbon Capture and Storage/Utilization

CDR: Carbon Dioxide Removal

PP: Polypropylene

K-SAR: Potassium Sarcosinate

TPMS: Triply Periodic Minimal Surface

LPS: Liter per Second

GPM: Gallon per Minute

SSA: Specific Surface Area

D_{L}: Diffusivity

K_{H}: Henry's Constant

$C_{\mathrm{CO_2}}$: CO_2 Concentration

$J_{\mathrm{CO_2}}$: CO_2 Flux

μ: Dynamic Viscosity

ρ: Liquid Phase Density

Acknowledgements

This research is supported by the US Department of Energy (DOE), Building Technologies Office and Laboratory Directed Research and Development and under Contract DE-AC05-00OR22725 with UT-Battelle LLC. This research used resources at the Building Technologies Research and Integration Center (BTRIC), a DOE Office of Science User Facilities operated by the Oak Ridge National Laboratory.

Data Availability Statement

The data that supports the findings of this study is available in the Supplementary Information.

References

1. H.-O. Pörtner, D.C.R., E.S. Poloczanska, K. Mintenbeck, M. Tignor, A. Alegría, M. Craig, S. Langsdorf, S. Löschke, V. Möller, A. Okem, *IPCC, 2022: Summary for Policymakers.* IPCC, 2022: p. 3-33.
2. Viebahn, P., A. Scholz, and O. Zelt, *The Potential Role of Direct Air Capture in the German Energy Research Program—Results of a Multi-Dimensional Analysis.* Energies, 2019. **12**(18).

3. Fuhrman, J., et al., *The role of direct air capture and negative emissions technologies in the shared socioeconomic pathways towards +1.5 °C and +2 °C futures.* Environmental Research Letters, 2021. **16**(11).
4. Beuttler, C., L. Charles, and J. Wurzbacher, *The Role of Direct Air Capture in Mitigation of Anthropogenic Greenhouse Gas Emissions.* Frontiers in Climate, 2019. **1**.
5. Ozkan, M., et al., *Current status and pillars of direct air capture technologies.* iScience, 2022. **25**(4): p. 103990.
6. Erans, M., et al., *Direct air capture: process technology, techno-economic and socio-political challenges.* Energy & Environmental Science, 2022. **15**(4): p. 1360-1405.
7. Fuhrman, J., et al., *Food–energy–water implications of negative emissions technologies in a +1.5 °C future.* Nature Climate Change, 2020. **10**(10): p. 920-927.
8. Deutz, S. and A. Bardow, *Life-cycle assessment of an industrial direct air capture process based on temperature–vacuum swing adsorption.* Nature Energy, 2021. **6**(2): p. 203-213.
9. Madhu, K., et al., *Understanding environmental trade-offs and resource demand of direct air capture technologies through comparative life-cycle assessment.* Nature Energy, 2021. **6**(11): p. 1035-1044.
10. Ellebracht, N.C., et al., *3D printed triply periodic minimal surfaces as advanced structured packings for solvent-based CO2 capture.* Energy & Environmental Science, 2023. **16**(4): p. 1752-1762.
11. *Direct Air Capture of CO2 with Chemicals*. 2011, American Physical Society(APS).
12. Mazzotti, M., et al., *Direct air capture of CO2 with chemicals: optimization of a two-loop hydroxide carbonate system using a countercurrent air-liquid contactor.* Climatic Change, 2013. **118**(1): p. 119-135.
13. Holmes, G. and D.W. Keith, *An air-liquid contactor for large-scale capture of CO2 from air.* Philos Trans A Math Phys Eng Sci, 2012. **370**(1974): p. 4380-403.
14. Keith, D.W., et al., *A Process for Capturing CO2 from the Atmosphere.* Joule, 2018. **2**(8): p. 1573-1594.
15. Wang, C., A.F. Seibert, and G.T. Rochelle, *Packing characterization: Absorber economic analysis.* International Journal of Greenhouse Gas Control, 2015. **42**: p. 124-131.
16. Abdullatif, Y., et al., *Emerging trends in direct air capture of CO(2): a review of technology options targeting net-zero emissions.* RSC Adv, 2023. **13**(9): p. 5687-5722.
17. McQueen, N., et al., *A review of direct air capture (DAC): scaling up commercial technologies and innovating for the future.* Progress in Energy, 2021. **3**(3).
18. Kasturi, A., et al., *An Effective Air-Liquid Contactor for CO2Direct Air Capture Using Aqueous Solvents.* Separation and Purification Technology, 2023.
19. Custelcean, R., *Direct Air Capture of CO2 Using Solvents.* Annu Rev Chem Biomol Eng, 2022. **13**: p. 217-234.
20. Brethomé, F.M., et al., *Direct air capture of CO2 via aqueous-phase absorption and crystalline-phase release using concentrated solar power.* Nature Energy, 2018. **3**(7): p. 553-559.
21. Custelcean, R., et al., *Direct Air Capture of CO2 with Aqueous Amino Acids and Solid Bis-iminoguanidines (BIGs).* Industrial & Engineering Chemistry Research, 2019. **58**(51): p. 23338-23346.
22. Al-Ketan, O. and R.K. Abu Al-Rub, *MSLattice: A free software for generating uniform and graded lattices based on triply periodic minimal surfaces.* Material Design & Processing Communications, 2020. **3**(6).
23. Darwish, O.M., *Effect of Saline Immersion and Freeze-Thaw Cycles on Performance of Fused Deposition Modelling Materials*, in *Mechanical Engineering*. 2019, University of Dayton.
24. Wilcox, J., et al., *Revisiting film theory to consider approaches for enhanced solvent-process design for carbon capture.* Energy & Environmental Science, 2014. **7**(5).

25. Kasturi, A., et al., *Carbon dioxide capture with aqueous amino acids: Mechanistic study of amino acid regeneration by guanidine crystallization and process intensification.* Separation and Purification Technology, 2021. **271**.
26. Sang Sefidi, V. and P. Luis, *Advanced Amino Acid-Based Technologies for CO2 Capture: A Review.* Industrial & Engineering Chemistry Research, 2019. **58**(44): p. 20181-20194.
27. Thee, H., et al., *A kinetic study of CO2 capture with potassium carbonate solutions promoted with various amino acids: Glycine, sarcosine and proline.* International Journal of Greenhouse Gas Control, 2014. **20**: p. 212-222.
28. Holmes, G., et al., *Outdoor Prototype Results for Direct Atmospheric Capture of Carbon Dioxide.* Energy Procedia, 2013. **37**: p. 6079-6095.
29. Sabatino, F., et al., *A comparative energy and costs assessment and optimization for direct air capture technologies.* Joule, 2021. **5**(8): p. 2047-2076.
30. McQueen, N., et al., *Cost Analysis of Direct Air Capture and Sequestration Coupled to Low-Carbon Thermal Energy in the United States.* Environ Sci Technol, 2020. **54**(12): p. 7542-7551.
31. Shayegh, S., V. Bosetti, and M. Tavoni, *Future Prospects of Direct Air Capture Technologies: Insights From an Expert Elicitation Survey.* Frontiers in Climate, 2021. **3**.
32. *Critical Surface Tension and Contact Angle with Water for Various Polymers*. 2023; Available from: https://www.accudynetest.com/polytable_03.html?sortby=contact_angle.
33. Wang, Z., et al., *Improved CO2 Absorption in a Gas–Liquid Countercurrent Column Using a Ceramic Foam Contactor.* Industrial & Engineering Chemistry Research, 2016. **55**(5): p. 1387-1400.
34. Weng, H., et al., *Performance characteristics of a new spherical metal mesh packing.* Chemical Engineering and Processing: Process Intensification, 2013. **72**: p. 68-73.
35. Wen, X., et al., *Development of a Novel Vertical-Sheet Structured Packing.* Chemical Engineering Research and Design, 2005. **83**(5): p. 515-526.
36. Bolton, S., et al., *3D printed structures for optimized carbon capture technology in packed bed columns.* Separation Science and Technology, 2019. **54**(13): p. 2047-2058.
37. Zeman, F., *Energy and material balance of CO2 capture from ambient air.* Environmental Science & Technology, 2007. **41**(21): p. 7558-7563.
38. Aronu, U.E., et al., *Kinetics of Carbon Dioxide Absorption into Aqueous Amino Acid Salt: Potassium Salt of Sarcosine Solution.* Industrial & Engineering Chemistry Research, 2011. **50**(18): p. 10465-10475.
39. Xiang, Q., et al., *Kinetics of the reversible reaction of CO2(aq) and HCO3(-) with sarcosine salt in aqueous solution.* J Phys Chem A, 2012. **116**(42): p. 10276-84.